Journal of Organometallic Chemistry 695 (2010) 558–566

Contents lists available at ScienceDirect

Journal of Organometallic Chemistry

journal homepage: www.elsevier.com/locate/jorganchem

Silver(I) and copper(I) complexes with ferrocenyl ligands bearing imidazole or pyridyl substituents

Susana Quintal [a], M. Concepción Gimeno [b], Antonio Laguna [b], Maria José Calhorda [a,*]

[a] Departamento de Química e Bioquímica, CQB, Faculdade de Ciências, Universidade de Lisboa, Campo Grande 1749-016 Lisboa, Portugal
[b] Departamento de Química Inorgánica, Instituto de Ciencia de Materials de Aragón, Universidad de Zaragoza-CSIC, E-50009 Zaragoza, Spain

ARTICLE INFO

Article history:
Received 7 September 2009
Received in revised form 10 November 2009
Accepted 11 November 2009
Available online 18 November 2009

Keywords:
Copper(I) complexes
Silver(I) complexes
Weak interactions
Ferrocenyl ligands
X-ray structures
DFT calculations

ABSTRACT

The reactions between five ferrocenyl derivatives containing both a C=O and at least an imidazole or pyridine nitrogen atom and $AgPF_6$, AgOTf, or $[Cu(NCCH_3)_4]PF_6$ precursors were studied. The ligand {[bis(2-pyridyl)amino]carbonyl}ferrocene (**L3**), derived from (2-pyridyl)amine, favored tetrahedral coordination of Ag^+ (with two ligands) and of Cu^+ (with two acetonitrile ligands left from the precursor). In all the other ligands, both metal centers coordinated linearly to two ligands, preferring the imidazole or pyridinic nitrogen to other nitrogen atoms (amine) or oxygen donors.

When the counter anions were triflate, the crystal structure showed a dimerization of the complex, with the ferrocenyl moieties occupying *cis* positions, by means of a weak Ag···Ag interaction. This was shown experimentally in the crystal structure of complex $[Ag(L1)_2]OTf$ (L1 = ferrocenyl imidazole) and in the presence of peaks corresponding to $\{Ag_2(L2)_3(OTf)\}^+$ and $\{Ag_2(L2)_4(OTf)\}^+$ in the mass spectra of $[Ag(L2)_2]OTf$ (L2 = ferrocenyl benzimidazole). In all complexes containing PF_6, there was no evidence for dimerization. Indeed, in the crystal structure of $[Ag(L2)_2]PF_6$, the ferrocenyl moieties occupy *trans* positions and the metal centers are far from each other. DFT calculations showed that the energy of the *cis* and *trans* conformers is practically the same and the balance of crystal packing forces leads to dimerization when triflate is present.

1. Introduction

The ferrocene molecule has been widely used in recent years as a building block for polynuclear complexes, polymers, supramolecular aggregates, and many other species exhibiting a wide range of properties [1]. The possibility of functionalizing easily one or both cyclopentadienyl rings opens the way to the synthesis of compounds, with applications in many areas, including optoelectronics, liquid crystals, electrochemical sensors, nanoparticles, catalysis, etc. [2–12].

The modest cytotoxic activity of the ferrocenium ion [13] was enhanced by modification of its environment [14]. Aminoacids and peptides were introduced in the rings in order to improve the interaction with biological targets, and the interactions with different metals, as well as application as sensors, were studied [15]. Ferrocenyl derivatives with nitrogen donor atoms in the ring substituents have been found to act as metalloligands towards a variety of metal centers, such as Rh(I) and Mo(II) [16,17], but mostly Cu(I), Ag(I), or Au(I) [18]. Sometimes helical [19] or double helical [20] structures are formed with d^{10} ions. Modification of the ligands may afford coordination polymers [21] or supramolecular structures [22]. In previous works we incorporated imidazole or benzimidazole units in ferrocene and tested the coordination capabilities of the new ligands toward molybdenum [17]. Some of these Fe–Mo complexes exhibited *in vitro* anti-tumor activity [17b], suggesting the potential interest of this kind of system combining molybdenum and iron, the two metals present in the most studied Fe–Mo nitrogenase. In this work, the coordination of the five ferrocenyl ligands shown in Scheme 1 to Ag(I) and Cu(I) was studied, affording new coordination modes, and different arrangements were found in the crystal structure depending on the ligand and the counter ion.

2. Results and discussion

The ligands ferrocenyl imidazole (**L1**), ferrocenyl benzimidazole (**L2**), {[bis(2-pyridyl)amino]carbonyl}ferrocene (**L3**), bis-ferrocenyl(2-aminopyridine) (**L4**), and ferrocenylamidobenzimidazole (**L5**) were prepared by the coupling reaction between FcCOCl [Fc = $(\eta^5\text{-}C_5H_5)Fe(\eta^5\text{-}C_5H_4)$] and the appropriate amine, namely imidazole, benzimidazole, dipyridylamine, 2-aminopyridine, and 2-aminobenzimidazole, respectively, in a 1:1 ratio, in dichloromethane and in the presence of NEt_3.

* Corresponding author. Tel.: +351 217 500 196; fax: +351 217 500 088.
E-mail address: mjc@fc.ul.pt (M.J. Calhorda).

0022-328X/$ - see front matter © 2009 Elsevier B.V. All rights reserved.
doi:10.1016/j.jorganchem.2009.11.013

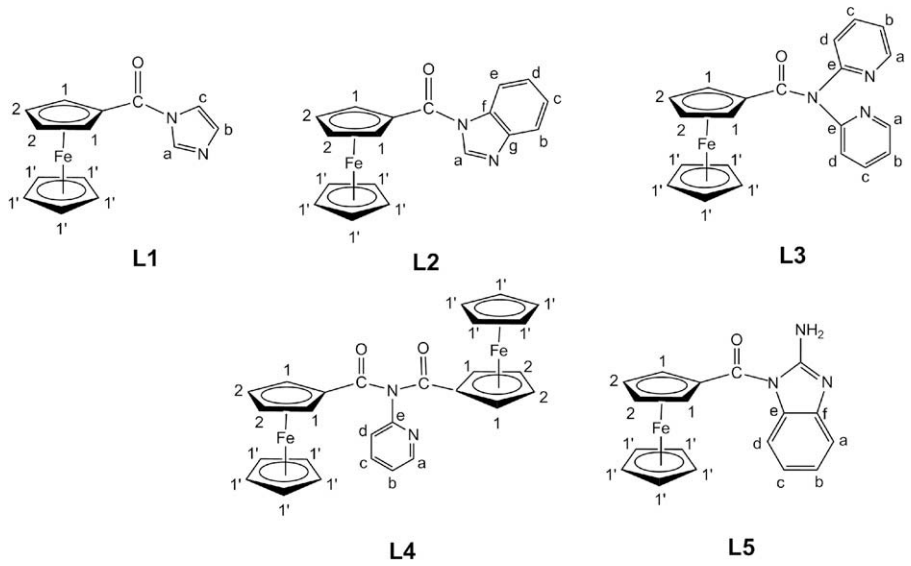

Scheme 1. The five metalloligands ligands studied, with the numbering scheme adopted.

Ligand **L1** reacted with $AgPF_6$ (1:1) forming a red solid (**C1**), with the ν(C=O) stretching frequency at 1690 cm^{-1}, shifted from 1680 cm^{-1} in the free ligand, and the ν(C=N) vibrational modes at 1378 and 1442 cm^{-1}. Typical vibrations assigned to C–H modes were also present. The ^1H NMR spectrum of **L1** in CD_2Cl_2 shows the signals of the imidazole ring protons: a singlet at 8.93 (Ha), and two doublets at 7.82 and 7.25 ppm, (Hc and Hb), with the Cp ring protons (H1′) at 4.35 ppm, and those of the substituted ring at 5.11 (H1) and 4.81 (H2) [17b]. Small deviations from the chemical shifts of the protons in the free **L1** were detected in **C1** (Ha 8.77, Hc 7.88, Hb 7.30), Cp ring (H1′ 4.35, H1 5.05, H2 4.81). The ^{13}C NMR spectrum of the complex displays eight peaks that could be assigned, by means of a HMQC correlation, to the imidazole carbon atoms (Ca 140.18, Cb 130.29, Cc 119.13), Cp ring (C1' 71.55, C1 72.45, C2 74.79, *C*(Cp)–C=O 70.41), and the C=O carbon at 168.98 ppm. Elemental analysis supported the formulation of this solid as $[Ag(L1)_2]PF_6$ (**C1**).

The reaction of the same ligand **L1** with AgOTf led to another red solid (**C1a**) with very similar NMR spectra (see Experimental section). The FTIR spectrum, on the other hand, showed two bands at 1700 and 1685 cm^{-1}, which can be assigned to ν(C=O) stretching modes. Single crystals suitable for X-ray diffraction studies were grown from a dichloromethane/*n*-hexane solution.

The mass spectra for complexes **C1** and **C1a** show the cation molecular peak $[Ag(L1)_2]^+$ at *m/z* = 666.98 as the most intense peak, and also the fragment $[Ag(L1)]^+$ at *m/z* = 386.95.

The crystal structure of complex **C1a** has been established by X-ray diffraction. The cation is shown in Fig. 1 and a selection of bond lengths and angles in Table 1. The structure consists of a dimer with two $[Ag(L1)_2]^+$ units bonded through Ag···Ag short distances of 2.9343(8) Å. The silver center is linearly coordinated by the nitrogen atoms of the imizadole rings; the geometry is slightly distorted with a N–Ag–N angle of 170.27(5)°, probably because the ligands point out of the planes formed by the N–Ag–N atoms. Also there is a very weak contact between the silver centers and one of the oxygens of the triflate group, Ag1–O4 2.879 Å. The Ag–N distances are 2.1188(15) and 2.1204(14) Å, which are of the same order than those found in complexes with the linearly coordinated silver atoms by imidazole ligands.

There are also several weak contacts between one of the oxygen of the triflate group, O4, and the protons H3, H12, and H16, which lie in the range 2.502(1)–2.582(1) Å, and can be considered as

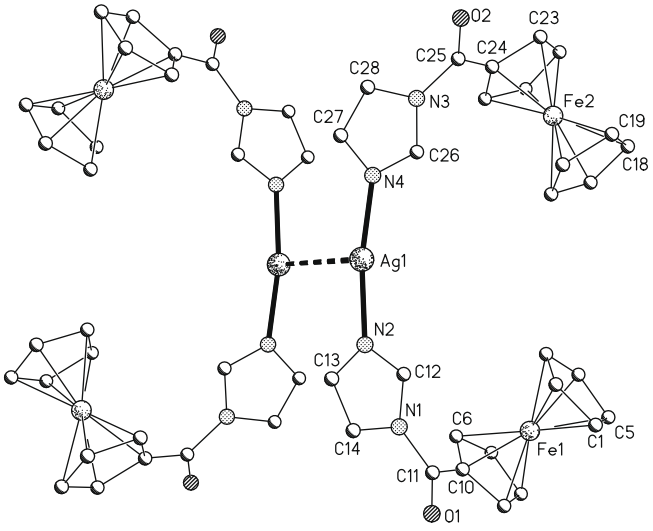

Fig. 1. Molecular diagram showing the overall structure of $[Ag_2(L1)_4]^{2+}$ (**C1a**) with the atomic notation scheme used.

Table 1
Selected bond lengths (Å) and angles (°) for complex **C1a**.

Ag(1)–N(4)	2.1188(15)	C(14)–N(1)	1.390(2)
Ag(1)–N(2)	2.1204(14)	C(24)–C(25)	1.454(2)
Ag(1)–Ag(1)#1	2.9342(8)	C(25)–O(2)	1.212(2)
C(11)–O(1)	1.206(2)	C(25)–N(3)	1.436(2)
C(11)–N(1)	1.434(2)	C(26)–N(4)	1.310(2)
C(12)–N(2)	1.308(2)	C(26)–N(3)	1.366(2)
C(12)–N(1)	1.366(2)	C(27)–C(28)	1.349(2)
C(13)–C(14)	1.351(2)	C(27)–N(4)	1.385(2)
C(13)–N(2)	1.387(2)	C(28)–N(3)	1.391(2)
N(4)–Ag(1)–N(2)	170.27(5)	C(12)–N(2)–C(13)	106.94(14)
N(4)–Ag(1)–Ag(1)#1	96.19(5)	C(12)–N(2)–Ag(1)	125.88(11)
N(2)–Ag(1)–Ag(1)#1	91.94(5)	C(13)–N(2)–Ag(1)	125.91(11)
O(1)–C(11)–N(1)	118.03(15)	O(2)–C(25)–N(3)	117.90(15)
N(1)–C(11)–C(10)	118.47(14)	C(26)–N(3)–C(28)	107.12(13)
N(2)–C(12)–N(1)	110.53(14)	C(26)–N(3)–C(25)	129.25(14)
C(12)–N(1)–C(14)	107.00(14)	C(28)–N(3)–C(25)	123.40(13)
C(12)–N(1)–C(11)	130.30(14)	C(26)–N(4)–C(27)	106.72(14)
C(14)–N(1)–C(11)	122.68(14)		

Symmetry transformations used to generate equivalent atoms:
#1 $-x+2$, $-y+1$, $-z+1$.

hydrogen bonds. These secondary interactions are shown in Fig. 2. The shortest hydrogen bond is the one formed by the carbonyl O2 oxygen and the proton H8, 2.392(1) Å, which connects these dimers with others.

The reactions between **L1** and $AgPF_6$ or AgOTf are represented in Scheme 2.

Reaction of ligand **L2** with $AgPF_6$ or AgOTf led to the formation of red solids (Scheme 3), which were identified as $[Ag(L2)_2]X$ (X = PF_6, **C2**; OTf, **C2a**). The ν(C=O) stretching modes of the ligand were observed at 1701 and 1696 cm^{-1} in the FTIR spectrum of **C2** and **C2a**, respectively (1674 cm^{-1} in free **L2**), and the characteristic modes of the Cp and benzimidazole rings were also present. The vibrational modes of the triflate were seen at 1289 ($\nu_{as(SO3)}$), 1026 ($\nu_{s(SO3)}$), 1223 ($\nu_{s(CF3)}$), and 1181 cm^{-1} ($\nu_{as(CF3)}$) for complex **C2a**. Peaks at 9.38, 8.31, 7.94 and 7.61 ppm in the ^1H NMR spectrum of **C2** in CD_2Cl_2 were assigned to the benzimidazole protons Ha, Hb, He and Hc + Hd, while those from the Cp and the substituted Cp are seen at 4.45 (H1′), 5.20 (H1) and 4.88 ppm (H2). The peaks of the carbon atoms in the ^{13}C NMR spectrum were assigned by performing HMQC spectra. The NMR spectra of complex **C2a** were very similar, with very small differences in chemical shifts.

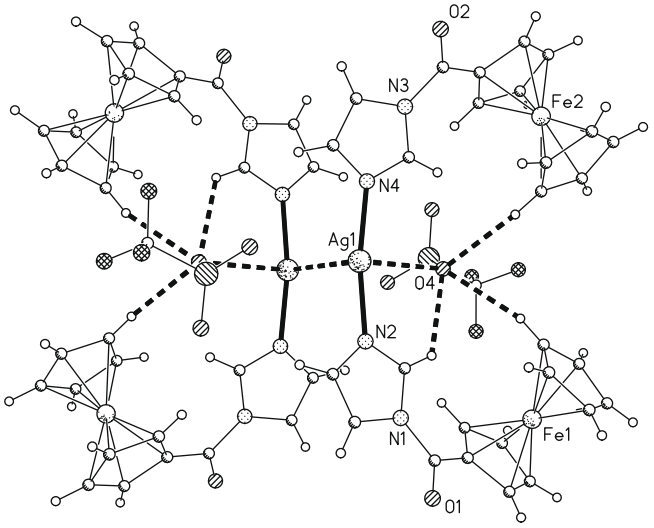

Fig. 2. Diagram of the dimeric molecule and the secondary bonds made by the oxygen of the triflate.

The mass spectrum of complex **C2** shows the cation molecular peak $[Ag(L2)_2]^+$ at m/z = 767.02 as the most intense peak. The mass spectrum of complex **C2a** shows the cation molecular peak $[Ag(L2)_2]^+$ at m/z = 767.02 as the most intense and the fragment $[Ag(L2)]^+$ at m/z = 436.97 (36%). Furthermore, other peaks, such as $\{Ag_2(L2)_3(OTf)\}^+$ at m/z = 1354.92 (12%) and $\{Ag_2(L2)_4(OTf)\}^+$ at m/z 1684.97 (6%), appear, indicating that the complex probably has a dimeric structure, as complex **C1a** in Fig. 1.

The structure of complex **C2** has been confirmed by X-ray diffraction studies performed on suitable crystals grown from a dichloromethane/diethyl ether solution. The cation is shown in Fig. 3. Selected bond lengths and angles are collected in Table 2. The silver atom lies in a symmetry center and consequently only half of the molecule corresponds to the asymmetric unit. The coordination around the silver center is linear with an ideal angle of 180° imposed by symmetry. The Ag–N distance is 2.122(3) Å, which is a similar value to that found in complex **C1a** (2.1188(15) and 2.1204(14) Å).

There are no silver···silver short contacts (see below). The fluorine atoms of the hexafluorophosphate group display several short contacts with CH hydrogen atoms. The shortest are 2.442(1) Å, F3···H18# (# $x-1, y, z$), and 2.506(1) Å, F1···H6, joining the two symmetry related molecules (Fig. 4).

$[Cu(NCCH_3)_4]PF_6$ also reacted with **L2** in dichloromethane to afford a red solid, which was identified as $[Cu(L2)_2]PF_6$ (**C2b**). The FTIR spectrum was almost superimposable with that of the Ag analogue (**C2**) and the elemental analysis supported this formulation. Unfortunately, the very low solubility prevented running any NMR spectra. The mass spectrum of complex **C2b** shows the cation molecular peak $[Cu(L2)_2]^+$ at m/z = 723 as the most intense.

The ligand **L3** is bidentate and therefore binds in a different way from the ligands **L1** and **L2**, which are monodentate. Reactions of ligand **L3** with $[Cu(NCCH_3)_4]PF_6$ and AgOTf were reported recently, and led to the formation of two complexes $[Cu(L3)_2]PF_6$ and [Ag(L3)]OTf, respectively [18i]. When $AgPF_6$ was used as a source for Ag^+, the tetracoordinate complex $[Ag(L3)_2]PF_6$ (**C3**) was formed. Ratios of 1:1 or 1:2 between metal and ligand **L3** led to the same complex. On the other hand, the reaction between $[Cu(NCCH_3)_4]PF_6$ and **L3** in 1:1 ratio led to the new complex $[Cu(L3)(NCCH_3)_2]PF_6$ (**C3a**, Scheme 4). In both complexes, the coordination of the ligand was attested by spectroscopic data. The FTIR

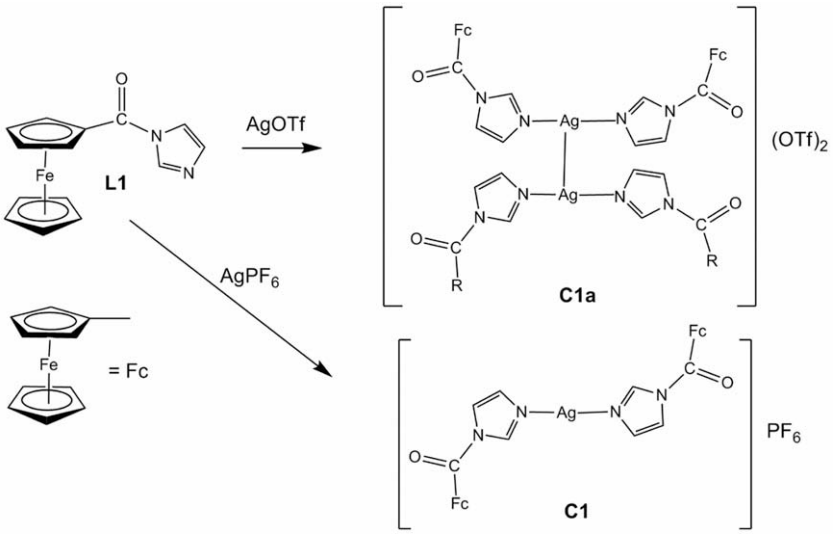

Scheme 2. Reactions between ligand **L1** and Ag^+ salts.

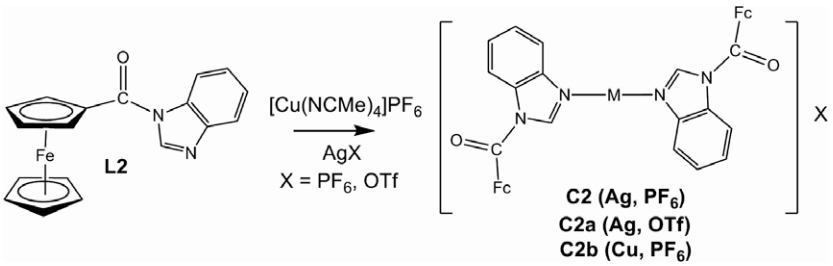

Scheme 3. Reactions between ligand **L2** and Cu^+ and Ag^+ precursors.

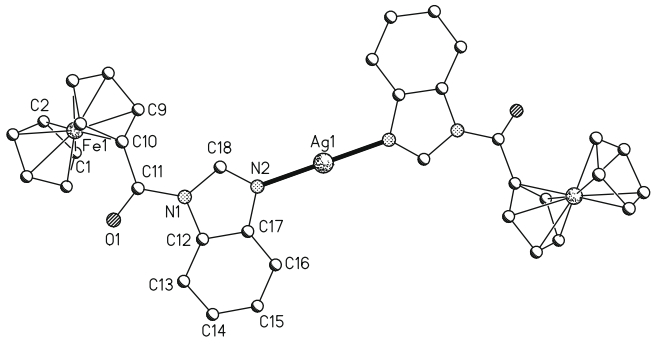

Fig. 3. Molecular diagram showing the overall structure of $[Ag(L2)_2]^{2+}$ (**C2**) with the atomic notation scheme used.

Table 2
Selected bond lengths (Å) and angles (°) for complex **C2**.

Ag(1)–N(2)	2.122(3)	N(1)–C(18)	1.381(4)
Ag(1)–N(2)#1	2.122(3)	N(1)–C(12)	1.409(4)
C(10)–C(11)	1.472(5)	C(12)–C(17)	1.402(4)
C(11)–O(1)	1.214(4)	C(17)–N(2)	1.402(4)
C(11)–N(1)	1.432(4)	N(2)–C(18)	1.302(4)
N(2)–Ag(1)–N(2)#1	180.000(1)	C(17)–C(12)–N(1)	104.9(3)
O(1)–C(11)–N(1)	118.8(3)	C(16)–C(17)–N(2)	129.2(3)
O(1)–C(11)–C(10)	124.7(3)	C(12)–C(17)–N(2)	109.2(3)
N(1)–C(11)–C(10)	116.5(3)	C(18)–N(2)–C(17)	106.9(3)
C(18)–N(1)–C(12)	106.9(3)	C(18)–N(2)–Ag(1)	131.2(2)
C(18)–N(1)–C(11)	128.1(3)	C(17)–N(2)–Ag(1)	121.2(2)
C(12)–N(1)–C(11)	124.8(3)	N(2)–C(18)–N(1)	112.1(3)
C(13)–C(12)–N(1)	133.2(3)		

Symmetry transformations used to generate equivalent atoms:
#1 $-x-1, -y+1, -z+1$ #2 $-x+1, -y, -z+1$.

spectra exhibited the most characteristic bands of the ligands, namely the ν(C=O) stretching at 1681 (**C3**) and 1680 (**C3a**) cm^{-1}. The ν(C≡N) vibrational modes were only observed at 2252 and 2267 cm^{-1} for **C3a**. ^1H NMR spectrum of **C3a** displays four peaks assigned to the four pyridyl protons in the range 7.57–8.58 ppm, a broad multiplet at 4.34 ppm from the two Cp rings, and a singlet at 2.17 ppm from the acetonitrile protons, integrating as 8:9:6. The peaks in the spectrum of **C3** are observed at very similar chemical shifts, and the Cp protons appear as a broad peak. Elemental analysis supports the proposed formulation.

The reaction between ligand **L4** and $[Cu(NCCH_3)_4]PF_6$ or $AgPF_6$ was also studied and led to two new complexes, $[Cu(L4)_2]PF_6$ (**C4a**) and $[Ag(L4)_2]PF_6$ (**C4**). The ν(C=O) and ν(C=N) modes in the FTIR spectrum give rise to several bands between 1676 and 1598 cm^{-1} for **C4**, and 1675–1561 cm^{-1} for **C4a**, indicating that the ligand is coordinated. In the free ligand, four well defined strong bands are visible. The low solubility of both complexes in common solvents led to low quality NMR spectra, but the presence of the peaks assigned to the pyridine protons at 7.37–8.46 ppm, and to the two kinds of Cp protons (4.36 ppm H1′, 4.48 ppm H1, H2) was confirmed in **C4**.

The geometries of the complexes should be as represented in Scheme 5, similar to the crystal structure of complex **C2** (Fig. 3), with the ligand **L2** binding through the pyridine nitrogen atom.

The mass spectra for these complexes show the cation molecular peaks for the silver derivative at $m/z = 1143$ ($[Ag(L4)_2]^+$, 35%) and for the copper species at $m/z = 1098.9$ ($[Cu(L4)_2]^+$, 100%); also the fragments at $m/z = 625$ ($[Ag(L4)]^+$, 100%) and at $m/z = 581$ ($[Cu(L4)]^+$, 25%) are present.

Several reactions between ligand **L5** and some Au^+ and Ag^+ precursors have already been reported [18h]. In particular, reaction with AgOTf yields the dimer $[Ag_2(L5)_4(OTf)_2]$, where the ligand acts as a monodentate ligand, using the benzimidazole nitrogen atom for coordination. The two anions act as bridges between two silver atoms, so that a distorted tetrahedral coordination is achieved around Ag, with two nitrogen and two oxygen atoms. On the other hand, Mo(II) complexes where the same ligand behaves as bidentate, using both the imidazole and the amine nitrogen atoms have also been described [17a].

In the absence of the triflate, it is expected that the reaction between **L5** and $AgPF_6$ will afford another linear complex with two ligands, $[Ag(L5)_2]PF_6$ (**C5**). The FTIR spectrum of **C5** shows several

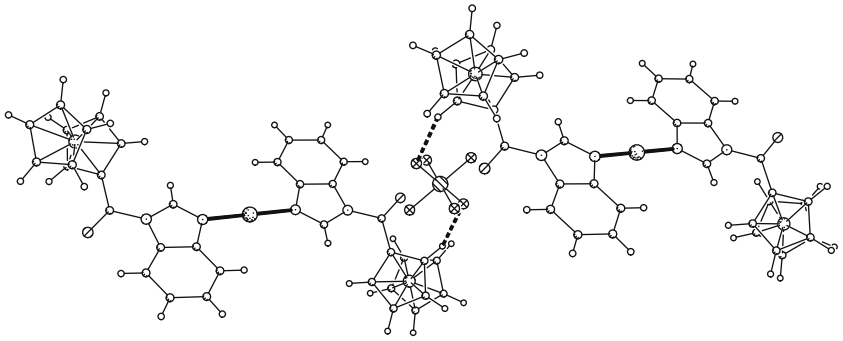

Fig. 4. Association of **C2** molecules through weak F···H interactions.

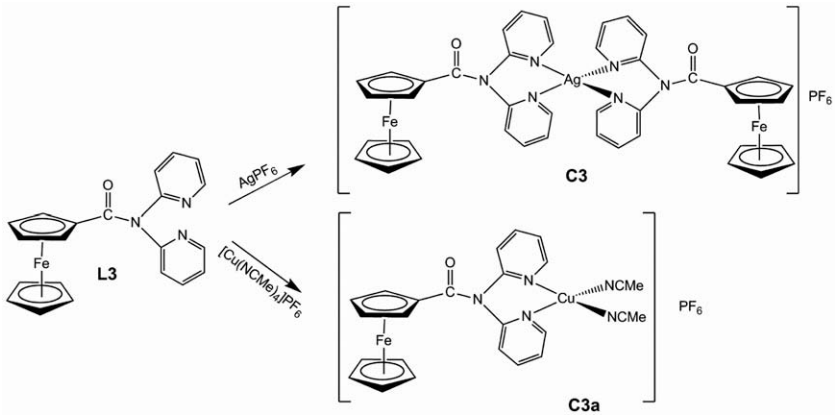

Scheme 4. Reactions between ligand **L3** and Cu(I) and Ag(I) precursors.

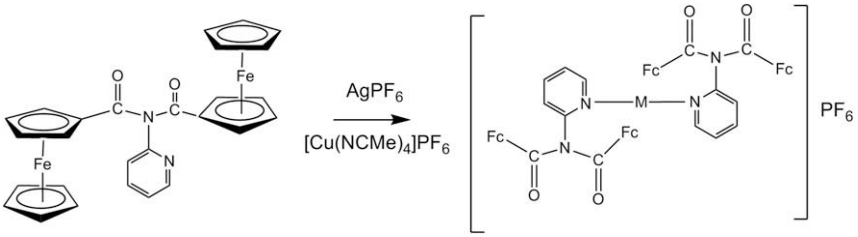

Scheme 5. Reactions between ligand **L4** and $[Cu(NCCH_3)_4]PF_6$ or $AgPF_6$.

bands assigned to the ν(N–H) stretching frequencies at 3431 cm^{-1}, and the ν(C=O) stretching at 1685 (**C5**) suggesting that the C=O and NH_2 groups remain non-coordinated, in contrast to what is observed in the Mo(II) complexes [17a]. The four benzimidazole protons appear as two doublets and two triplets, at 7.42, 7.27, 7.12, and 7.06 ppm in the ^1H NMR spectrum, the five protons of the Cp at 4.34 ppm, the protons of the substituted Cp at 4.99 and 4.72, and the NH_2 at 6.83 ppm.

The reaction with $[Cu(NCCH_3)_4]PF_6$ leads to the formation of a complex with a FTIR spectrum very similar to that of **C5**, $[Cu(L5)_2]PF_6$ (**C5a**), with the ν(N–H) stretching frequencies at 3416 cm^{-1}, and the ν(C=O) stretching 1684 cm^{-1}, indicating that these groups are not coordinated.

The mass spectrum of complex **C5a** shows the cation molecular peak $[Cu(L5)_2]^+$ at $m/z = 753$ as the most intense peak (see Scheme 6).

The reactions described suggest that Cu(I) and Ag(I) prefer almost always the linear coordination, the only exception being observed with ligand **L3**. This ligand is bidentate with two nitrogen donor atoms that will form a six-membered ring when chelating the metal. Both **L4** [17b] and **L5** [17a] can act as bidentate, but **L4** has one oxygen as donor atom (too hard to bind easily the soft d^{10} metal centers), while **L5** gives rise to a more strained four-membered ring. Since a linear coordination is a favored one for these cations, these two ligands remain monodentate.

Another interesting result concerns the dimerization, leading to weak Ag···Ag interactions, which was observed with the triflate counter anion. This is evident in the crystal structure of complex **C1a** and strongly suggested in the mass spectra of complex **C2a.** This type of dimerization is probably made difficult by the bulkiness of ligands **L4** and **L5**.

2.1. DFT calculations

DFT calculations [23] (ADF program [24]; see details in Computational section) were performed in **C1** and **C2** in order to explore some of the factors which may favor dimerization. In the crystal structures, the substituents are *cis* oriented in the dimer (Fig. 1) and *trans* in the monomer (Fig. 3).

The geometry of the two monomers (to be called **C1m** and **C2m**, for clarity) was optimized under C_i symmetry for the *trans* isomers, C_s symmetry for the *cis* isomer of **C2m**, and no symmetry for the other *cis* isomer (**C1m**). The symmetry of this species is very close to C_s symmetry, as can be seen in Fig. 5. For the smaller complex **C1a** the geometry of the dimer (**C1d**) was also optimized to estimate the interaction energy between the two silver atoms.

The energies of both isomers are very close; *trans*-**C1m** is more stable than *cis*-**C1m** by 4.21 kcal mol^{-1}, and *trans*-**C2m** than *cis*-**C2m** by 0.12 kcal mol^{-1}.

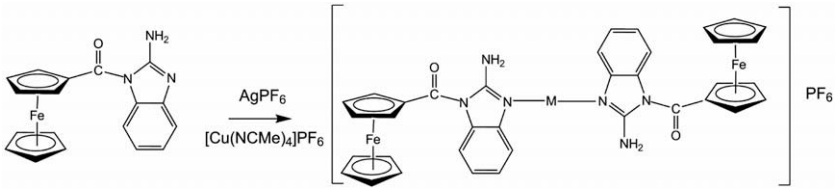

Scheme 6. Reactions between ligand **L5** and $[Cu(NCCH_3)_4]PF_6$ or $AgPF_6$.

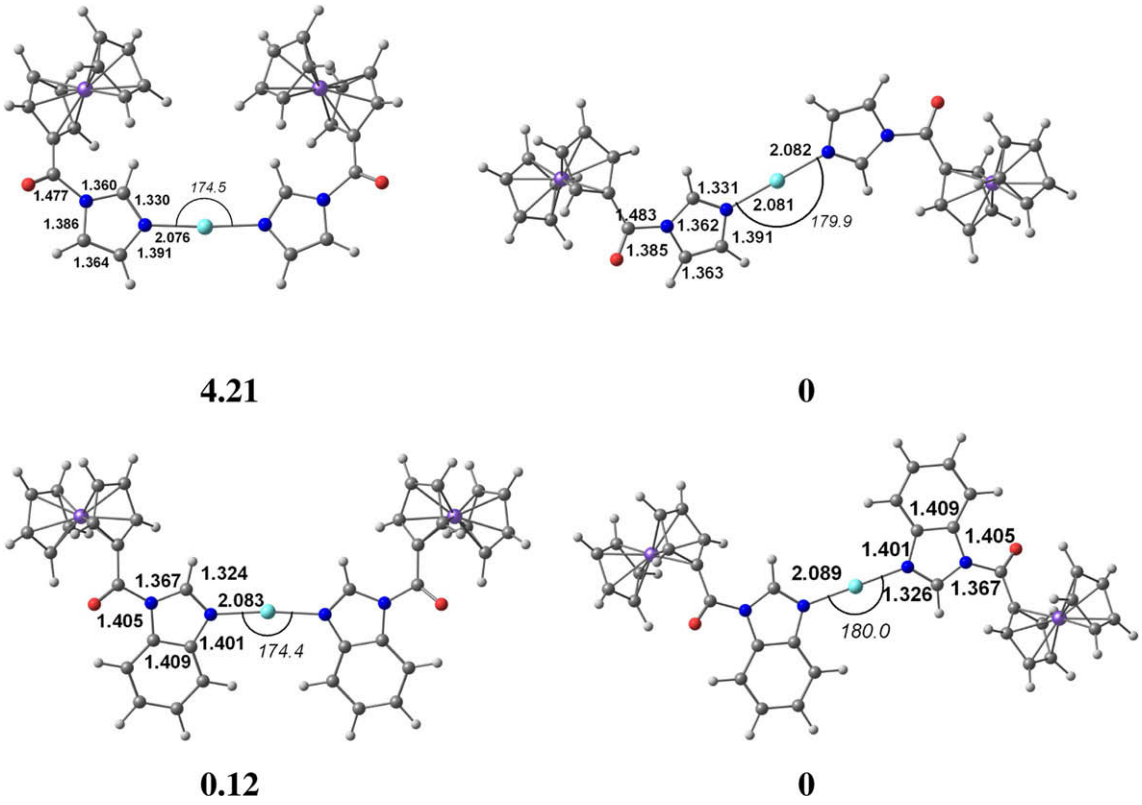

Fig. 5. Optimized geometries of the monomers **C1m** (top) and **C2m** (bottom) in the *cis* and *trans* arrangements and relative energies (kcal mol^{-1}).

These results indicate that the *trans* isomers are more stable than the *cis*, though the difference is extremely small in the benzimidazole derivative. Although the *cis* conformation is required to form the dimer, this energy difference is not the determining factor. When the geometry of the dimer of **C1m** is optimized, the energy is higher than twice the energy of **C1m**. This is not a surprising result, since the two monomers are cationic, and suggests that the anions play a relevant role. On the other hand, DFT calculations are not adequate for describing this weak argentophilic interaction, which has been widely studied [25]. Unfortunately, a reliable calculation taking into account the anions is outside the scope of our possibilities. Still, combining these with the experimental results, we can conclude that the triflate anion can build three dimensional structures where the Ag monomers dimerize leading to a more stable structure, while with the hexafluorophosphate anion the monomers lead to the most stable crystal structure.

3. Conclusions

The five ligands ferrocenyl imidazole (**L1**), ferrocenyl benzimidazole (**L2**), {[bis(2-pyridyl)amino]carbonyl}ferrocene (**L3**), bis-ferrocenyl(2-aminopyridine) (**L4**), and ferrocenylamidobenzimidazole (**L5**) reacted with the Ag^+ and Cu^+ precursors to afford complexes where only nitrogen atoms bound the metals. While **L3** led to tetrahedral species, $[Ag(L3)_2]^+$ or $[Cu(L3)(NCCH_3)_2]^+$, the other ligands favored a linear coordination of the metal centers. When the counter ion was triflate, the $[ML_2]^+$ monomers dimerized with formation of a weak Ag···Ag interaction, while this never occurred in the presence of the PF_6 anion, and the monomers were observed in the crystal structure. DFT calculations showed that the *cis* or *trans* conformation of the ferrocenyl moiety in the monomer did not influence the energy, and is not the factor responsible for the dimerization, which is probably induced by the crystal packing forces acting together.

4. Experimental

4.1. Chemical studies

Commercially available reagents and all solvents were purchased from standard chemical suppliers. Solvents were dried using common procedures. Syntheses of copper complexes were carried out under nitrogen atmosphere using Schlenk techniques. Mass spectra were recorded with a VG Autospec, with the ESI+ (electrospray) technique.

The ligands ferrocenyl imidazole (**L1**) [17b], ferrocenyl benzimidazole(**L2**) [17b], {[bis(2-pyridyl)amino]carbonyl}ferrocene (**L3**) [18i], bis-ferrocenyl(2-aminopyridine) (**L4**) [26] and ferrocenylamidobenzimidazole (**L5**) [18h], were prepared, as reported, by the coupling reaction between FcCOCl [Fc = (η^5-C_5H_5)Fe(η^5-C_5H_4)] and the appropriate amine, namely imidazole, benzimidazole, dipyridylamine, 2-aminopyridine, and 2-aminobenzimidazole, respectively, in a 1:1 ratio, in dichloromethane and in presence of NEt_3. The complex $[Cu(NCCH_3)_4]PF_6$ were prepared as described in the literature [27].

Infrared spectra were measured on a Mattson 7000 FT spectrometer. Samples were run as KBr pellets. NMR spectra were recorded on a Bruker Avance-400 spectrometer in dmso-d_6 or CD_2Cl_2. Elemental analyses were carried out at University of Vigo, Spain.

4.2. $[Ag(L1)_2]PF_6$ (**C1**)

$AgPF_6$ (0.2 mmol, 0.0504 g) in ethanol (10 ml) was added to a solution (CH_2Cl_2, 10 ml) of L1 (0.2 mmol, 0.056 g). The red solution was left in the dark overnight and a red precipitate was formed, filtered off washed with 3 × 10 ml of diethyl ether and dried under vacuum. Yield: 0.064 g, 78.8%.

Elemental Anal. Calc. for **C1** ($C_{28}H_{24}N_4O_2PF_6Fe_2Ag$): C, 41.36; H, 2.97; N, 6.89. Found: C, 41.39; H, 2.98; N, 6.85%.

^{1}H NMR (400 MHz, CD_2Cl_2, r.t): δ = 8.77 (m, Ha, 1H), 7.88 (m, 1H, Hc), 7.30 (m, 1H, Hb), 5.05 (m, 2H, H1), 4.81 (m, H2, 2H), 4.35 (s, 5H, H1′) ppm.

^{13}C NMR (100.6 MHz, CD_2Cl_2, r.t.): δ = 168.98 (C=O), 140.18 (Ca), 130.29 (Cb), 119.13 (Cc), 74.79 (C2), 72.45 (C1), 71.55 (C1′), 70.41 (*C*(Cp)–C=O) ppm.

4.3. $[Ag_2(L1)_4](OTf)_2$ (**C1a**)

AgOTf (0.2 mmol, 0.0514 g) in CH_2Cl_2 (5 ml) was added to a solution (CH_2Cl_2, 10 ml) of L1 (0.2 mmol, 0.056 g). A red solution was formed. The stirring was continued for 4 h and then *n*-hexane was added. After a few days in the fridge, red crystals were filtered off, washed with 3 × 10 ml of *n*-hexane and dried under vacuum. Suitable crystals were selected for X-ray diffraction studies. Yield: 0.051 g, 63.0%.

Elemental Anal. Calc. for **C1a** ($C_{58}H_{48}N_8O_{10}S_2F_6Fe_4Ag_2$): C, 42.63; H, 2.96; N, 6.86; S, 3.92. Found: C, 42.32; H, 2.87; N, 6.79; S, 3.86%.

^{1}H NMR (400 MHz, CD_2Cl_2, r.t.): δ = 8.99 (m, 1H, Ha), 7.84 (m, 1H, Hc), 7.30 (m, 1H, Hb), 5.07 (m, 2H, H1), 4.79 (m, 2H, H2), 4.36 (s, 5H, H1′) ppm.

^{13}C NMR (100.6 MHz, CD_2Cl_2, r.t.): δ = 168.92 (C=O), 140.73 (Ca), 130.21 (Cb), 118.84 (Cc), 74.66 (C2), 72.51 (C1), 71.53 (C1′), 70.58 (*C*(Cp)–C=O) ppm.

4.4. $[Ag(L2)_2]PF_6$ (**C2**)

$AgPF_6$ (0.2 mmol, 0.0504 g) in ethanol (10 ml) was added to a solution (CH_2Cl_2, 10 ml) of L2 (0.2 mmol, 0.033 g). The red solution was left in the dark overnight and red crystals were formed, filtered off, washed with 3 × 10 ml of diethyl ether and dried under vacuum. Suitable crystals were selected for X-ray diffraction studies. Yield: 0.078 g, 81.8%.

Elemental Anal. Calc. for **C2**·0.5CH_2Cl_2 ($C_{36.5}H_{29}N_4O_2ClPF_6Fe_2Ag$): C, 45.89; H, 3.06; N, 5.86. Found: C, 45.85; H, 2.92; N, 6.02%.

^{1}H NMR (400 MHz, CD_2Cl_2, r.t.): δ = 9.38 (s, 1H, Ha), 8.31 (m, 1H, Hb), 7.94 (m, 1H, He), 7.61 (m, 2H, Hc + Hd), 5.20 (m, 2H, H1), 4.88 (m, 2H, H2), 4.45 (s, 5H, H1′) ppm.

^{13}C NMR (100.6 MHz, CD_2Cl_2, r.t.): δ = 170.02 (C=O), 145.74 (Ca), 145.15 (Cg), 131.87 (Cf), 127.54 (Cc), 126.60 (Cd), 119.43 (Ce), 116.62 (Cb), 74.89 (C2), 72.92 (C1), 71.83 (C1′) ppm.

4.5. $[Ag(L2)_2]OTf$ (**C2a**)

AgOTf (0.2 mmol, 0.0514 g) in CH_2Cl_2 (5 ml) was added to a solution (CH_2Cl_2, 10 ml) of L2 (0.2 mmol, 0.056 g). The red solution was left in the dark overnight and red crystals were formed, filtered off, washed with 3 × 10 ml of diethyl ether and dried under vacuum. Yield: 0.069 g, 72.0%.

Elemental Anal. Calc. for **C2a**·0.5CH_2Cl_2 ($C_{37.5}H_{29}N_4O_5ClSF_3Fe_2Ag$): C, 46.93; H, 3.05; N, 5.84; S, 3.34. Found: C, 47.09; H, 2.93; N, 6.06; S, 3.43%.

^{1}H NMR (400 MHz, CD_2Cl_2, r.t.): δ = 9.60 (s, 1H, Ha), 8.33 (m, 1H, Hb), 7.94 (m, 1H, He), 7.59 (m, 2H, Hc + Hd), 5.18 (m, 2H, H1), 4.81 (m, 2H, H2), 4.40 (s, 5H, H1′) ppm.

^{13}C NMR (100.6 MHz, CD_2Cl_2, r.t.): δ = 170.18 (C=O), 145.45 (Ca), 141.48 (Cg), 132.06 (Cf), 127.25 (Cc), 126.38 (Cd), 119.55 (Ce), 116.60 (Cb), 74.45 (C2), 72.61 (C1), 71.64 (*C*(Cp)–C=O), 71.43 (C1′) ppm.

4.6. $[Cu(L2)_2]PF_6$ (**C2b**)

$[Cu(NCCH_3)_4]PF_6$ (0.5 mmol, 0.186 g) in CH_2Cl_2 (5 ml), L2 (0.5 mmol, 0.165 g) was added, under stirring and N_2 and a red precipitate was formed. The stirring was continued overnight. The precipitate was filtered off, washed with 3 × 10 ml of ethanol and dried under vacuum. Yield: 0.153 g, 64.3%.

Elemental Anal. Calc. for **C2b**·CH_2Cl_2($C_{37}H_{30}N_4O_2Cl_2PF_6Fe_2Cu$): C, 46.60; H, 3.17; N, 5.87. Found: C, 47.29; H, 3.09; N, 6.47%.

NMR: poor solubility in common NMR solvents.

4.7. $[Ag(L3)_2]PF_6$ (**C3**)

To a solution (ethanol, 10 ml) of $AgPF_6$ (0.2 mmol, 0.0504 g), a solution (dichloromethane, 2 ml) of L3 (0.4 mmol, 0.154 g) was added. After a few minutes some crystals precipitated. The reaction was continued for 2 days and then the suspension was filtered and the solid washed with 3 × 10 ml of diethyl ether and dried under vacuum. Yield: 0.1710 g, 77.5%.

Elemental Anal. Calc. for **C3**·CH_2Cl_2 ($C_{43}H_{36}N_6O_2Cl_2PF_6Fe_2Ag$): C, 46.77; H, 3.29; N, 7.61. Found: C, 46.07; H, 2.99; N, 7.95%.

^{1}H NMR (400 MHz, CD_2Cl_2, r.t.): δ = 8.45 (d, 2H, Ha), 8.04 (t, 2H, Hc), 7.64 (d, 2H, Hd), 7.52 (t, 2H, Hb), 4.54 (br, H1′, 9H, H1/H2) ppm.

^{13}C NMR (100.6 MHz, CD_2Cl_2, r.t.): δ = 171.53 (C=O), 153.70 (Ce), 151.03 (Ca), 141.50 (Cc), 125.96 (Cd), 125.38 (Cb), 73.01 (very br, C1, C2, C1′) ppm.

4.8. $[Cu(L3)(NCCH_3)_2]PF_6$ (**C3a**)

To a solution (dichloromethane, 10 ml) of $[Cu(NCCH_3)_4]PF_6$ (0.5 mmol, 0.186 g), a solution (dichloromethane, 5 ml) of L3, (0.5 mmol, 0.192 g) was added, under stirring and N_2. An orange solution was formed. The stirring was continued for 2 h and then the solution was concentrated and *n*-hexane was added. After a few days in the fridge, a yellow precipitate was filtered off, washed with 3 × 10 ml of *n*-hexane and dried under vacuum. Yield: 0.249 g, 74.0%.

Elemental Anal. Calc. for **C3a** ($C_{25}H_{23}N_5OPF_6FeCu$): C, 44.56; H, 3.44; N, 10.39. Found: C, 44.25; H, 3.27; N, 8.84%.

^{1}H NMR (400 MHz, CD_2Cl_2, r.t.): δ = 8.58 (br, 2H, Ha), 8.01 (br, 2H, Hc), 7.67 (br, 2H, Hd), 7.57 (br, 2H, Hb), 4.34 (m, br, 9H, H1′, H1/H2), 2.17 (s, 6H, CH_3CN) ppm.

^{13}C NMR (HMQC, CD_2Cl_2, r.t.): δ = 149.69 (Ca), 140.75 (Cc), 126.62 (Cd), 125.50 (Cb), 72.80 (C1, C2, C1'), 2.83 (*C*H_3CN) ppm.

4.9. $[Ag(L4)_2]PF_6$ (**C4**)

$AgPF_6$ (0.2 mmol, 0.0504 g) in ethanol (10 ml) was added to a solution (CH_2Cl_2, 10 ml) of L4 (0.4 mmol, 0.207 g). The red solution was left in the dark overnight and red precipitate were formed, filtered off washed with 3 × 10 ml of diethyl ether and dried under vacuum. Yield: 0.192 g, 60.2%.

Elemental Anal. Calc. for **C4**·4CH_2Cl_2 ($C_{58}H_{52}N_4O_4Cl_8PF_6Fe_4Ag$): C, 43.60; H, 3.28; N, 3.51. Found: C, 42.84; H, 3.14; N, 3.86%.

^{1}H NMR (400 MHz, dmso-d_6, r.t.): δ = 8.46 (d, 1H, Ha), 7.90 (t, 1H, Hc), 7.35 (t, 1H, Hb), 7.29 (d, 1H, Hb,), 4.48 (m, 8H, H1/H2), 4.36 (s, 10H, H1′) ppm.

4.10. $[Cu(L4)_2]PF_6$ (**C4a**)

To a solution (dichloromethane, 3 ml) of $[Cu(NCCH_3)_4]PF_6$ (0.5 mmol, 0.186 g), a solution (dichloromethane, 5 ml) of L4 (0.5 mmol, 0.259 g) was added, under stirring and N_2. A red precipitate was formed. The stirring was continued for 2 h and a red pre-

cipitate was filtered off, washed with 3 × 10 ml of diethyl ether and dried under vacuum. Yield: 0.307 g, 82.1%.

Elemental Anal. Calc. for **C4a**·$3CH_2Cl_2$ ($C_{57}H_{50}N_4O_4Cl_6PF_6Fe_4Cu$): C, 45.65; H, 3.36; N, 3.74. Found: C, 44.75; H, 3.73; N, 4.08%.

NMR: poor solubility in common NMR solvents.

4.11. $[Ag(L5)_2]PF_6$ (**C5**)

$AgPF_6$ (0.2 mmol, 0.0504 g) in ethanol (10 ml) was added to a solution (CH_2Cl_2, 10 ml) of L5 (0.4 mmol, 0.138 g). The red solution was left in the dark overnight and a red precipitate was formed, filtered off washed with 3 × 10 ml of diethyl ether and dried under vacuum. Yield: 0.128 g, 67.9%.

Elemental Anal. Calc. for **C5** ($C_{36}H_{30}N_6O_2PF_6Fe_2Ag$): C, 45.84; H, 3.21; N, 8.91. Found: C, 44.22; H, 3.28; N, 8.48%.

^{1}H NMR (400 MHz, CD_2Cl_2, r.t): δ = 7.42 (d, Ha, 1H), 7.27 (t, 1H, Hb), 7.12 (d, 1H, Hd), 7.06 (t, 1H, Hc), 6.83 (s, 2H, NH_2), 4.99 (m, 2H, H1), 4.72 (m, 2H, H2), 4.34 (s, H1', 4H) ppm.

^{13}C NMR (100.6 MHz, CD_2Cl_2, r.t.): δ = 172.99 (C═O), 155.54 (C–NH_2), 139.52(Ce), 130,77. (Cf), 125.12 (Cb), 122.33 (Cc), 115.47 (Ca), 114.97 (Cd), 73.75 (C2), 73.23 (C(Cp)–C═O), 73.18 (C1), 71.83 (C1′) ppm.

4.12. $[Cu(L5)_2]PF_6$ (**C5a**)

To a solution (dichloromethane, 3 ml) of $[Cu(NCCH_3)_4]PF_6$ (0.1 mmol, 0.037 g), a solution (dichloromethane, 5 ml) of L5, (0.2 mmol, 0.069 g) was added, under stirring and N_2. A red solution was formed. The stirring was continued for 2 days and a red precipitate was filtered off, washed with 3 × 10 ml of *n*-hexane and dried under vacuum. Yield: 0.059 g, 62.7%. Elemental Anal. Calc. for **C5a**·$0.5C_6H_{14}$ ($C_{39}H_{37}N_6O_2PF_6Fe_2Cu$): C, 49.73; H, 3.96; N, 8.92. Found: C, 49.69; H, 3.65; N, 9.16%.

NMR: poor solubility in common NMR solvents.

Table 3
X-ray data for complexes **C1a** and **C2**.

Compound	C1a	C2
Formula	$C_{29}H_{24}AgF_3Fe_2N_4O_5S$	$C_{36}H_{28}AgF_6Fe_2N_4O_2P$
M_r	817.15	913.16
Habit	Orange prism	Orange needle
Crystal size (mm)	0.40 × 0.25 × 0.15	0.28 × 0.06 × 0.05
Crystal system	Triclinic	Triclinic
Space group	$P\bar{1}$	$P\bar{1}$
Cell constants:		
a (Å)	6.6375(13)	6.3448(13)
b (Å)	13.402(3)	10.216(2)
c (Å)	16.324(3)	12.577(3)
α (°)	82.87(3)	77.97(3)
β (°)	83.11(3)	83.83(3)
γ (°)	89.82(3)	84.40(3)
V (Å^3)	1430.4(5)	790.3(3)
Z	2	1
D_x (Mg m^{-3})	1.897	1.919
μ (mm^{-1})	1.820	1.649
F (0 0 0)	816	456
T (°C)	−130	−130
$2\theta_{max}$	52	50
No. of reflections		
Measured	21 990	5003
Independent	5598	2702
Transmissions	0.529–0.771	0.465–0.92
R_{int}	0.016	0.018
Parameters	406	238
Restraints	0	0
wR (F^2, all Refl.)	0.047	0.065
R (F, >4σ(F))	0.018	0.031
S	1.049	1.054
Max. $\Delta\rho$ (e Å^{-3})	0.337	0.941

4.12.1. Crystal structure determinations

Data were registered on an Oxford Diffraction Xcalibur diffractometer. The crystals were mounted in inert oil on glass fibers and transferred to the cold gas stream of the diffractometer. Data were collected using monochromated Mo Kα radiation (λ = 0.71073) in ω scans. Absorption corrections based on multiple scans were applied with the program SADABS. The structures were solved by direct methods and refined on F^2 using the program SHELXL-97 [28]. All non-hydrogen atoms were refined anisotropically. Hydrogen atoms were included using a riding model. Further crystal data are given in Table 3.

4.12.2. DFT calculations

Density Functional Theory calculations (DFT) [23] were performed using the Amsterdam Density Functional program package (ADF) [24]. Gradient corrected geometry optimizations [29] (gas-phase and solvent) were performed without symmetry constraints, or with the symmetry referred in the text, using the Local Density Approximation of the correlation energy (Vosko-Wilk-Nusair) [30] augmented by the exchange–correlation functional of Becke and Perdew (BP86) [31]. Triple-ζ Slater-type orbitals (STO) were used to describe the valence shells of N, C, O, H, and Ag, with a set of two polarization functions (p,f for Ag; d,f for N, C, O and p,d for H). The core orbitals were frozen for Ag ([1–3]s, [2–3]p, [3]d), N, C, and O (1s). The relativistic effects were treated with the ZORA approximation [32].

Acknowledgements

S.Q. thanks FCT for a postdoctoral fellowship (SFRH/BPD/11463/2002) and M.J.C. thanks FCT, POCI, and FEDER (project PPCDT/QUI/58925/2004). M.C.G. and A.L. thank the Dirección General de Investigación Científica y Técnica (CTQ2007-67273-C02-01) for financial support.

Appendix A. Supplementary material

CCDC 743979 and 743980 contain the supplementary crystallographic data for complexes **C1a** and **C2**. These data can be obtained free of charge from The Cambridge Crystallographic Data Center via www.ccdc.cam.ac.uk/data_request/cif. Supplementary data associated with this article can be found, in the online version, at doi:10.1016/j.jorganchem.2009.11.013.

References

[1] A. Togni, T. Hayashi (Eds.), Ferrocenes, Homogeneous Catalysis, Organic Synthesis and Materials Science, VCH, Weinheim, 1995.
[2] A. Togni, R.L. Halterman (Eds.), Metallocenes, VCH, Weinheim, 1998.
[3] N.J. Long, Metallocenes, Blackwell, Oxford, 1998.
[4] N.J. Long, Angew. Chem., Int. Ed. 34 (1995) 21–38.
[5] I. Manners, Adv. Organomet. Chem. 37 (1995) 131–168.
[6] I. Manners, Chem. Commun. (1999) 857–865.
[7] Y. Zhu, O. Clot, M.O. Wolf, G.P.A. Yap, J. Am. Chem. Soc. 120 (1998) 1812–1821.
[8] P.D. Beer, Acc. Chem. Res. 31 (1998) 71–80.
[9] P.D. Beer, P.A. Gale, G.Z. Chen, J. Chem. Soc., Dalton Trans. (1999) 1897–1909.
[10] R.V. Honeychuck, M.O. Okoroafor, L.H. Shen Jr., Organometallics 5 (1986) 482–490.
[11] A.C. Templeton, M.P. Wuelfing, R.W. Murray, Acc. Chem. Res. 33 (2000) 27–36.
[12] R.S. Ingram, M.J. Hostetler, R.W. Murray, J. Am. Chem. Soc. 119 (1997) 9175–9178.
[13] (a) H. Tamura, M. Miwa, Chem. Lett. (1997) 1177–1178;
(b) D. Osella, M. Ferrali, P. Zanello, F. Laschi, M. Fontani, C. Nervi, G. Cavigiolo, Inorg. Chim. Acta 306 (2000) 42–48;
(c) L.V. Popova, V.N. Babin, Y.A. Beleusov, Y.S. Nekrasov, A.E. Snegireva, N.P. Borodina, G.M. Shaposhnikova, O.B. Bychenko, P.M. Raevskii, M.N. Morozova, A.I. Ilyna, K.G. Shitkov, Appl. Organomet. Chem. 7 (1993) 85–94;
(d) L.V. Snegur, A.A. Simenel, Y.S. Nekrasov, E.A. Morozova, Z.A. Starikova, S.M. Peregudova, Y.V. Kuzmenko, V.N. Babin, L.A. Ostrovskaya, N.V. Bluchterova, M.M. Fomina, J. Organomet. Chem. 689 (2004) 2473–2497;
(e) V.N. Babin, P.M. Raevskii, K.G. Snchitkov, L.V. Snegur, Y.S. Nekrasov, Rossiiskii Khimicheskii Zhurnal 39 (1995) 19–29.

[14] (a) A. Vessières, S. Top, P. Pigeon, E. Hillard, L. Boubeker, D. Spera, G. Jaouen, J. Med. Chem. 48 (2005) 3937–3940;
(b) J. Rajput, J.R. Moss, A.T. Hutton, D.T. Hendricks, C.E. Arendse, C. Imrie, J. Organomet. Chem. 689 (2004) 1553–1568;
(c) S. Top, A. Vessières, G. Leclercq, J. Quivy, J. Tang, J. Vaisserman, M. Huché, G. Jaouen, Chem. Eur. J. 9 (2003) 5223–5236.
[15] (a) D.R. van Staveren, N. Metzler-Nolte, Chem. Rev. 104 (2004) 5931–5985;
(b) S.I. Kirin, D. Wissenbach, N. Metzler-Nolte, New J. Chem. 29 (2005) 1168–1173;
(c) O. Brosh, T. Weyhermüller, N. Metzler-Nolte, Inorg. Chem. 38 (1999) 5308–5313;
(d) X. Hatten, T. Weyhermüller, N. Metzler-Nolte, J. Organomet. Chem. 689 (2004) 4856–4867;
(e) A. Hess, O. Brosh, T. Weyhermüller, N. Metzler-Nolte, J. Organomet. Chem. 589 (1999) 75–84;
(f) S. Chowdhury, K.A. Mahmoud, G. Schatte, H.-B. Kraatz, Org. Biomol. Chem. 3 (2005) 3018–3023;
(g) F.E. Appoh, T.C. Sutherland, H.-B. Kraatz, J. Organomet. Chem. 689 (2004) 4669–4677;
(h) F.E. Appoh, T.C. Sutherland, H.-B. Kraatz, J. Organomet. Chem. 690 (2005) 1209–1217;
(i) O. Brosh, T. Weyhermüller, N. Metzler-Nolte, Eur. J. Inorg. Chem. (2000) 323–330;
(j) K. Heinze, M. Schlenker, Eur. J. Inorg. Chem. (2004) 2974–2988;
(k) K. Heinze, M. Beckmann, Eur. J. Inorg. Chem. (2005) 3450–3457;
(l) H. Shinoara, T. Kusaka, E. Yokota, R. Monden, M. Sisido, Sens. Actuators, B 65 (2000) 144–146;
(m) C. Suksai, P. Leeladee, D. Jainuknan, T. Tuntulani, N. Muangsin, O. Chailapakul, P. Kongsaeree, C. Pakavatchai, Tetrahedron Lett. 46 (2005) 2765–2769;
(n) A. Berduque, G. Herzog, Y.E. Watson, D.W.M. Arrigan, O. Reynes, G. Royal, E. Saint-Aman, Electroanalysis 17 (2005) 392–399;
(o) H. Miyaji, G. Gasser, S.J. Green, Y. Molard, S.M. Strawbridge, J.H.R. Tucker, Chem. Commun. (2005) 5355–5357.
[16] J. Rajput, A.T. Hutton, J.R. Moss, H. Su, C. Imrie, J. Organomet. Chem. 691 (2006) 4573–4588.
[17] (a) P.N. Martinho, S. Quintal, P. Costa, S. Losi, V. Félix, M.C. Gimeno, A. Laguna, M.G.B. Drew, P. Zanello, M.J. Calhorda, Eur. J. Inorg. Chem. (2006) 4096–4103;
(b) S. Quintal, J. Matos, I. Fonseca, V. Félix, M.G.B. Drew, N. Trindade, M. Meireles, M.J. Calhorda, Inorg. Chim. Acta 361 (2008) 1584–1596.
[18] (a) B. Bildstein, M. Malaun, H. Kopacka, K. Wurst, M. Mitterböck, K.-H. Organia, G. Opromolla, P. Zanello, Organometallics 18 (1999) 4325–4336;
(b) B. König, M. Nimtz, H. Zieg, Tetrahedron 22 (1995) 6267–6272;
(c) E.M. Barranco, O. Crespo, M.C. Gimeno, P.G. Jones, A. Laguna, M.D. Villacampa, J. Organomet. Chem. 592 (1999) 258–264;
(d) R. Pastene, H. LeBozec, S.A. Moya, Inorg. Chem. Commun. 3 (2000) 376–378;
(e) E.M. Barranco, M.C. Gimeno, A. Laguna, M.D. Villacampa, Inorg. Chim. Acta 358 (2005) 4177–4182;
(f) H. Hou, G. Li, Y. Son, Y. Fan, Y. Zhu, L. Zhu, Eur. J. Inorg. Chem. (2003) 2325–2332;
(g) D.G. MacDonald, J.F. Corrigan, Dalton Trans. (2008) 5048–5053;
(h) M.J. Calhorda, P.J. Costa, P.N. Martinho, M.C. Gimeno, A. Laguna, S. Quintal, M.D. Villacampa, J. Organomet. Chem. 691 (2006) 4181–4188;
(i) J.E. Aguado, O. Crespo, M.C. Gimeno, P.G. Jones, A. Laguna, Y. Nieto, Eur. J. Inorg. Chem. (2008) 3031–3039.
[19] B. Quidonoz, G. Labat, H. Stoeckli-Evans, A. Von Zelewsky, Inorg. Chem. 43 (2004) 7994–8004.
[20] (a) J.E. Aguado, M.J. Calhorda, P.J. Costa, O. Crespo, V. Félix, M.C. Gimeno, P.G. Jones, A. Laguna, Eur. J. Inorg. Chem. (2004) 3038–3047;
(b) C. Fang, C. Duan, H. Mo, C. He, Q. Meng, Y. Liu, Y. Mei, Z. Wang, Organometallics 20 (2001) 2525–2532.
[21] (a) T. Mochida, K. Okazawa, Dalton Trans. (2006) 693–704;
(b) R. Horikoshi, T. Mochida, H. Moriyama, Inorg. Chem. 41 (2002) 3017–3024;
(c) D.L. Reger, K.J. Brown, J.R. Gardinier, M.D. Smith, Organometallics 22 (2003) 4973–4983.
[22] (a) E.M. Barranco, O. Crespo, M.C. Gimeno, P.G. Jones, A. Laguna, Eur. J. Inorg. Chem. (2004) 4820–4827;
(b) T. Mochida, F. Shimizu, H. Shimizu, K. Okazawa, F. Sato, D. Kuwahara, J. Organomet. Chem. 692 (2007) 1834–1844;
(c) D. Braga, M. Polito, D. D'Addario, E. Tavigliani, D.M. Proserpio, F. Grepioni, J.W. Stead, Organometallics 22 (2003) 4532–4538.
[23] R.G. Parr, W. Yang, Density Functional Theory of Atoms and Molecules, Oxford University Press, New York, 1989.
[24] (a) G. te Velde, FM. Bickelhaupt, S.J.A. van Gisbergen, C.F. Guerra, E.J. Baerends, J.G. Snijders, T. Ziegler, J. Comput. Chem. 22 (2001) 931–967;
(b) C.F. Guerra, J.G. Snijders, G. te Velde, E.J. Baerends, Theor. Chem. Acc. 99 (1998) 391–403;
(c) ADF2007, SCM, Theoretical Chemistry, Vrije Universiteit, Amsterdam, The Netherlands <http://www.scm.com>.
[25] (a) S. Riedel, P. Pyykkö, R.A. Mata, H.-J. Werner, Chem. Phys. Lett. 405 (2005) 148–152;
(b) E.J. Fernández, A. Laguna, J.M. López-de-Luzuriaga, M. Monge, P. Pyykkö, N. Runeberg, Eur. J. Inorg. Chem. (2002) 750–753.
[26] S. Quintal, M.J. Calhorda, in preparation.
[27] G.J. Kubas, Inorg. Synth. 19 (1979) 90–91.
[28] G.M. Sheldrick, SHELXL-97, A Program for Crystal Structure Refinement, University of Göttingen, 1997.
[29] (a) L. Versluis, T. Ziegler, J. Chem. Phys. 88 (1988) 322–328;
(b) L. Fan, T. Ziegler, Chem. Phys. 95 (1991) 7401–7408.
[30] S.H. Vosko, L. Wilk, M. Nusair, Can. J. Phys. 58 (1980) 1200–1211.
[31] (a) A.D. Becke, J. Chem. Phys. 88 (1988) 1053–1062;
(b) J.P. Perdew, Phys. Rev. B 33 (1986) 8822–8824;
(c) J.P. Perdew, Phys. Rev. B 34 (1986) 7406.
[32] E. van Lenthe, A. Ehlers, E. Baerends, J. Chem. Phys. 110 (1999) 8943–8953.